J. Fluid Mech. (1967), *vol.* 29, *part* 2, *pp.* 273–287
Printed in Great Britain

Two-dimensional incompressible fluid jet penetration

By D. F. HOPKINS
Douglas Aircraft Company, Santa Monica, California
AND J. M. ROBERTSON
Department of Theoretical and Applied Mechanics, University of Illinois, Urbana

(Received 1 September 1966 and in revised form 28 February 1967)

The principal characteristics of jet penetration are the appearance of free streamlines at the sides of the jet and of a dividing streamline, which separates the jet and penetrated fluid. Kinematic analysis of such flow via free-streamline theory and the notched hodograph is developed with one unspecified parameter, the ratio of jet to counterstream velocity in the steady flow case. The kinetics of the problem, appearing when the jet and penetrated (or counterstream) fluid differ in density, is simply related to the kinematic solution via the square root of the density ratio. Experiments, both steady state and transient with several liquids, are presented which generally verify the theory. The experiments also yield information on the magnitude of the parameter and indicate its variation with the density ratio.

1. Introduction

Fluid jet penetration involves the dynamic interaction of a high velocity stream of fluid with a broader, slower-moving body of fluid into which or through which the jet moves. The penetration occurrence may appear as a transient phenomenon with the jet impinging on and then penetrating into an essentially quiescent body of liquid, or the penetrated fluid body may be moving towards the jet at just the proper speed so that a steady-state process appears. During the penetration process, the jet is deflected by this opposing fluid, which in deflecting the jet is also deformed. Thus, fluid from two different sources interacts and solid boundaries are not directly involved. In the region of penetration, an interface or dividing streamline is formed between jet and penetrated fluid. This interface is sharply defined at the tip of the jet but becomes less distinct in the wake region of the deflected jet where mixing and mass transfer between the two regions occur. The main problem of jet penetration is to determine the shape of the interface and its location at subsequent intervals of time. The phenomenon is similar to the direct impingement of two jets; indeed, if one of the impinging jets is increased in width towards infinity, the process then becomes that of jet penetration.

A jet may penetrate into a fluid of the same density (if not composition), into a fluid of different density, or even into a plastic medium. Early studies involved

the penetration of a fuel injection spray into air as reported by Miller & Beardsley (1926) and continued by Lee (1932) with experiments on the penetration into water and glycerine. Many stratified fluid flows appear in the form of jets of a heavier fluid flowing under a lighter one. Thus meteorologists are interested in the flow of cold air under warmer (lighter) air at a front, and in the flow of a mixture of loose snow or of dust in air. The oceanographer is interested in density currents in which sediment laden water flows down the canyons off the continental shelf, or from stream into reservoirs. In another entirely different area of interest, jet penetration theory was formulated during World War II in connection with the penetration of armour plate by the high velocity jet from a lined charge. Presumably due to the high speed of action, the penetrated medium was successfully treated as a fluid. This work was reported by Birkhoff, MacDougall, Pugh & Taylor (1948) and Pack & Evans (1951) and later extended experimentally by Eichelberger (1956) and Singh (1957). Ehrich (1953) has analysed the penetration of jets obliquely into a stream, while Rao (1958) studied an air jet blowing into a counterflow of air with measurements of the mean flow and turbulence patterns. A jet of cooling fluid blowing forward from the nose of a body into super- and hypersonic flows has been considered and studied experimentally by Stalder & Inouye (1956), Warren (1960), Romeo & Sterrett (1963) and Baron & Alzner (1963). Recently, Wuest & von Trotha (1964) have employed an analysis similar to that presented in this paper to determine appropriate body contours for such applications. Interaction of forward blowing jets with the bow shock of a re-entry vehicle as a means of control was investigated by Charczenko & Hennessey (1961). In another consideration Banks & Chandrasekhara (1963) studied the hole produced in the surface of water by an impinging air jet. This study has been continued by Banks & Bhavamai (1965) with liquid jets.

The present study, although furnishing information relevant to all of the above noted cases of jet penetration, is limited to the analytical and experimental study of incompressible fluid jet penetration during the period—or in the flow region—for which the penetrating and penetrated fluids are effectively separated by an interface, i.e. viscous or turbulent mixing across the dividing streamline is ignored.

Examples of jet penetration are depicted in figure 1. Thus, in the first stage of surface penetration (figure 1*a*), the jet as it moves through space encounters the surface of a liquid body. The tip of the jet is split and deflected back, and the surface of the liquid is deformed at the point of impact. As the jet continues to penetrate, the vertex of the interface (dividing streamline DS) between the two fluids moves progressively deeper into the body of fluid, as sketched in figure 1*b*, with the jet now horizontal. Cavities defined by the free streamlines (FS) are formed on either side of the deflected jet as it is turned back. Initially, these are open to the atmosphere, but, as penetration progresses, they collapse near the surface, and trapped vortices are established on either side of the jet. When the jet penetrates into a countersteam, it impinges directly into fluid moving in a direction opposite to that of the jet. The jet is split and deflected back, and the deflected portion is swept downstream with the counterflow. If the proper counterflow velocity U is chosen, the position of the interface DS is stationary.

The flow pattern is symmetrical about the axis of the jet. Realistically, the jet cannot originate at infinity, but a nozzle must be located reasonably close to the penetration zone.

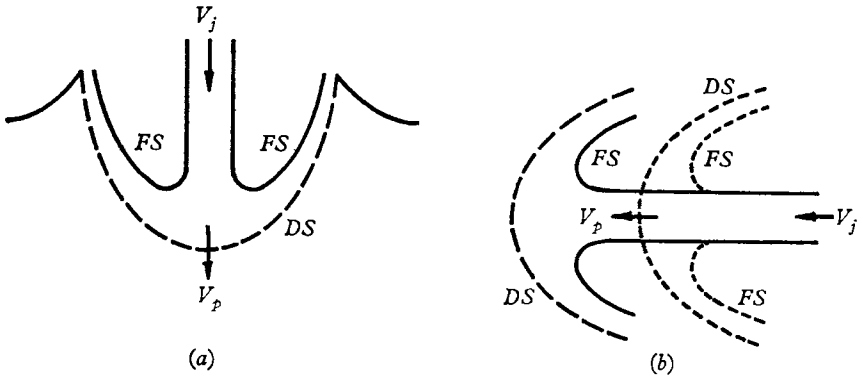

FIGURE 1. Examples of jet penetration flows: (*a*) near liquid surface, (*b*) stages of unsteady penetration.

2. Analytical flow model

Analytical treatment of jet penetration flow requires a simplified model which adequately represents the physical occurrence. The following characteristics of the penetration process are used to develop such a model.

(*a*) No solid boundaries are involved in the flow. Although the jet is necessarily generated by a nozzle, this may be located out of the region of interest.

(*b*) Boundary or shear layers at the interfaces between the several fluids are unimportant.

(*c*) The lateral spread of the dividing streamline is limited.

The development of a flow model is based on the hydrodynamic theory of ideal fluids. It is assumed that the fluids involved are inviscid and incompressible and that gravity and surface tension forces may be neglected. In the analysis, the flow is taken to be plane two-dimensional; the problem may thus be treated by the powerful methods of complex variables and conformal mapping.

The penetration process as conceived in this model is shown in the z-plane of figure 2. A plane two-dimensional jet originates from a source at positive infinity and penetrates into a counterstream originating at minus infinity. The jet velocity is taken as V directed to the left and the counterstream velocity as U to the right. A stagnation point occurs at the origin O; the centre streamlines in the jet and the stream divide to form the jet-stream interface (dividing streamline DS) OC. A recirculation region appears on either side of the jet and is bounded by free streamline (FS) $BMNA$. With this flow model, the problem now is to determine the shape of the streamlines and the pressure and velocity fields in the jet and the counterstream. Birkhoff & Caywood (1949) solved this problem via the Helmholtz free-streamline theory. Strict adherence to this theory admits only one possible situation; the velocity of the jet must be equal to the velocity of the stream, i.e. $V = U$. In the resulting flow pattern, the jet-stream interface (DS)

spread is unlimited, and an infinitely wide cavity or dead water region ($W = \infty$) occurs. This contradicts the experimental observations of the penetration phenomenon, characteristics (*c*) above. As in the analysis of cavity flows past bluff bodies (see Robertson 1965, p. 471), a more realistic solution is obtained by allowing the free streamline velocity to differ from that of the uniform stream. In the present application, such a flow model yields a finite spread of the *DS*, as desired.

The free streamline then becomes parallel to the horizontal axis at point N; along the streamline from B to N the speed is taken constant and equal to the

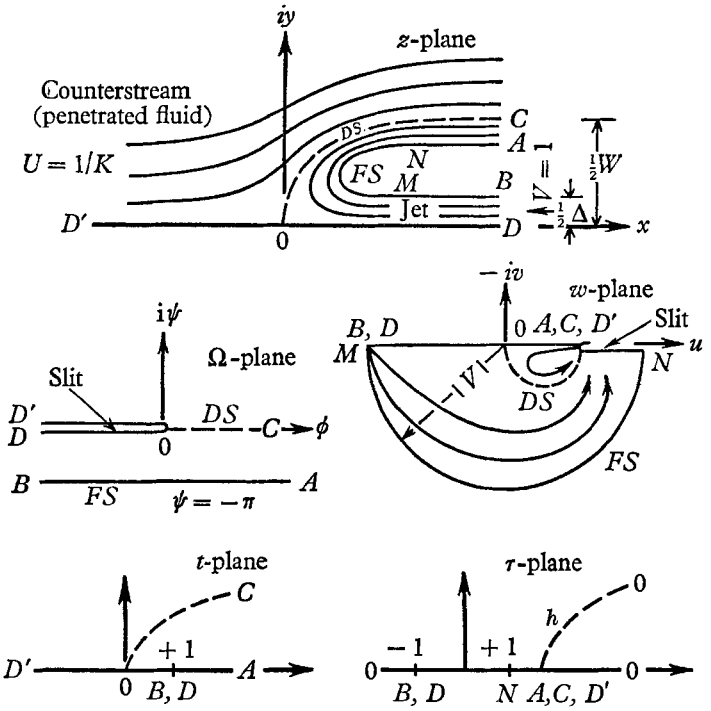

FIGURE 2. Jet penetration depiction in the several mapping planes.

magnitude of the jet velocity, V. At infinity downstream, however, the streamlines in the external flow become parallel, and the velocity along FS at point A must be equal to U, the approach velocity of the counterstream. Thus, from N to A along the parallel segment of the free streamline, the velocity must decrease from V to U. Physically, this decrease in velocity is attributed to the effects of viscosity and turbulence in the wake region, as suggested by Roshko (1954). Specifically, the notched hodograph, or dissipation, model is adopted for this analysis as detailed in the following paragraphs.

The flow in the physical plane is symmetrical about the real axis, and only the upper half is considered in the mapping. To further facilitate the mapping, the velocity is normalized so that $V = 1$, and the half-width of the jet is taken to be $\Delta/2 = \pi$. This normalization in no way reduces the generality of the solution. Since U is less than V, we let $V/U = 1/U = K$. Representation of the problem in the

several mapping planes involved is indicated in figure 2. Certain characteristics of the flow in the physical z-plane are known. Thus, at negative and positive infinity the streamlines of the counterstream are parallel, and the velocity is equal to $U = 1/K$. At positive infinity, the width $\Delta = 2\pi$ of the incoming jet is known, and its velocity is $V = 1$. The deflected portion of the jet reaches velocity $U = 1/K$ at positive infinity. Along the free streamline from B to N, the velocity is constant in magnitude and is equal to the jet velocity. From N to A the direction of the free streamline is parallel to the axis of the jet, but the velocity magnitude decreases from $V = 1$ to $U = 1/K$.

From the characteristics of the flow in the z-plane, the free streamline and the dividing streamline can be mapped in the complex potential plane, $\Omega = \phi + i\psi$. The value of ψ is taken to be zero along the symmetry and DS streamlines, $D'OD$ and OC respectively. These map into the real axis of the complex potential plane with $D'OD$ bent around a semi-infinite slit on the negative real axis. Along the free streamline $BMNA$, $\psi = -\pi$. Thus, in the Ω-plane the flow consists of the upper half plane and a lower strip of width π. The hodograph plane, of the complex velocity $w = u - iv$, is also easily mapped. The constant-velocity free streamline BMN maps into a semicircle of unit radius with the complete flow field appearing inside it. Streamlines $D'OD$ and the segment NA of the free streamline form the real axis of the w-plane. The free streamline segment NA appears as a short slit in the boundary of the semicircle. This type of hodograph is thus often referred to as a 'notched hodograph'.

The Ω-plane can be mapped on to the upper half of an auxiliary t-plane, shown at the bottom of figure 2, via the Schwarz–Christoffel transformation which gives

$$\Omega = t + \ln(1-t). \tag{1}$$

In the w-plane the flow is inside the semicircle; the interior of this can be mapped on the upper half of a τ-plane, also shown in figure 2, by the well known Joukowsky transformation, thus

$$2\tau = w + (1/w). \tag{2}$$

At points A, C, D' the complex velocity is real and equal to U. Since $U = 1/K$, these points are located on the real axis at

$$h = \frac{1}{2}\left(\frac{1}{K} + K\right) = \frac{K^2+1}{2K}. \tag{3}$$

The linear fractional Moebius transformation is used to complete the solution by relating t and τ.

$$t = -\frac{h+1}{\tau - h}. \tag{4}$$

The mapping is complete, the functions $\Omega = \Omega(w)$ and $z = z(w)$ can now be found by substitution. Thus from (1), (2) and (4)

$$\Omega(w) = -\frac{2w(h+1)}{(w-K)(w-1/K)} + \ln\left[\frac{(w+1)^2}{(w-K)(w-1/K)}\right]. \tag{5}$$

This determines the complete flow pattern in the hodograph plane.

To determine the streamlines in the z-plane, the $z = z(w)$ relation must be found. From (1)

$$d\Omega = \frac{t}{t-1}\,dt.$$

By substituting the expressions for t and τ from (4) and (2) and noting $w = d\Omega/dz$

$$dz = \frac{4(h+1)^2(w-1)}{(w+1)(w^2-2wh+1)^2}\,dw. \tag{6}$$

Integration and simplification leads to the following equation:

$$z = 2(h+1) - \frac{2(h+1)}{w^2-2hw+1} - \ln\frac{(w+1)^2}{w^2-2hw+1} - \frac{K+1}{K-1}\ln\frac{w-K}{K(Kw-1)}, \tag{7}$$

which maps the w-plane onto the z-plane. This, along with (5), constitutes the solution for the flow in the physical plane. It has not been possible to eliminate w between (5) and (7) to obtain $\Omega(z)$ and the equations for $\Omega(w)$ and $z(w)$ are thus retained as representing the solution in parametric form.

3. Comparison with Wuest & von Trotha solution

This same problem has been solved by Wuest & von Trotha (1964), but for a more general occurrence. Their solution is achieved via a technique dubbed the 'Blasius–Prandtl hodograph method' (see Robertson 1965, pp. 352, 445), in which identification of the singularities in the hodograph plane is followed by the integration $z = \int (1/w)\,d\Omega$ to find the $z(\Omega)$ relation. This same method was also outlined in the more complete work (Hopkins 1962) upon which this paper is based. In the Wuest & von Trotha work, a doubly notched hodograph is employed so that not only is the velocity magnitude along the free streamline (represented by the radius of the circle) allowed to exceed the velocity U of the approach counterstream, but also the issuing jet velocity is considered to be less in magnitude than that along the free streamline. This requires the fluid speed along the FS to increase between B and M to the free-streamline magnitude just as between N and A it decreases to U. The latter expectation or requirement is common to the present dissipation-model notched hodograph and usually rationalized as resulting from energy dissipation in the flow downstream of the immediate region of interest. However, it is not possible to justify the velocity increase between B and M for the doubly notched hodograph, since this requires an energy increase in the flow direction. Thus, the more general nature of the Wuest & von Trotha solution is physically unrealistic and their solution indications involving this velocity increase are not significant.

When the Wuest & von Trotha analysis is limited to the single notch, their velocity ratio V_l/V_m is unity. In that case their figure 12 indicates the variation in the x locations of the leading points of the DS and FS streamlines as summarized for the present study in figure 3. For the range in K considered here, their figure 12 indicates results at K values of about 1·05, 1·43 and 2·0 which agree with the theoretical values of the present study to within the precision with which it was possible to read their figure.

4. Some calculated flow patterns

The complete flow field, including the shapes of the dividing streamline DS and free streamline FS, is obtainable from (5) and (7). The FS is of particular interest when the jet is being used at the front of a body, since this streamline defines a contour for the body nose which will maintain a constant pressure along the surface. Similarly, DS defines the penetration interface of jets shooting into other fluids.

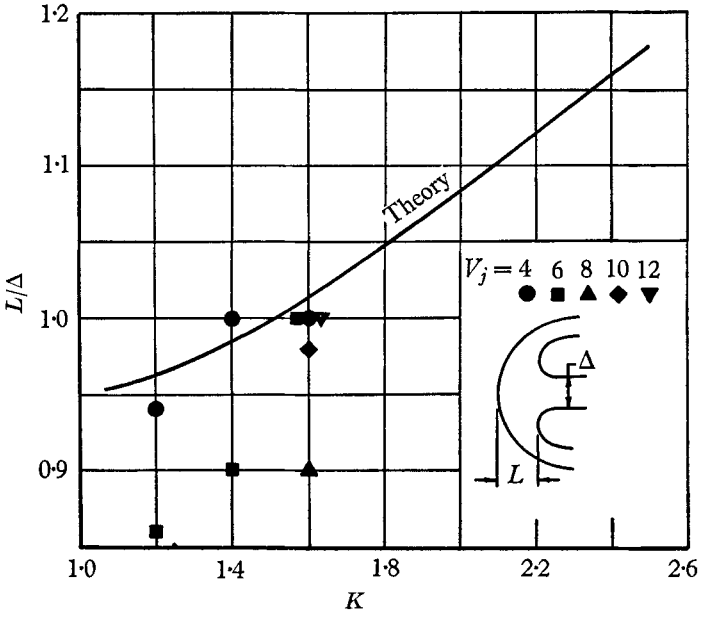

FIGURE 3. Variation of the leading distance L/Δ with parameter K.

To plot the streamlines in the physical plane, the flow pattern in the w-plane must first be determined. The expression for the complex potential (5) is broken up into its real and imaginary parts and the imaginary part is

$$\psi = \arctan\left[\frac{-2(u^2-v^2-2hu+1)(v+uv)-2(u^2-v^2+2u+1)(hv-uv)}{(u^2-v^2+2u+1)(u^2-v^2-2hu+1)-4(v+uv)(hv-uv)}\right] + \frac{2(h+1)[v(u^2-v^2-2hu+1)+2u(hv-uv]}{(u^2-v^2-2hu)^2+4(hv-uv)^2}. \quad (8)$$

For a constant value of ψ, the equation relates the velocity components, u and v, along the streamline. A different flow pattern is obtained for each value of the parameter K via the factor h as specified by (3).

The above equation for $\psi = \psi(u, v)$ is implicit in u and v, and it is not possible to assign a value to ψ and solve directly for the values of u and v which satisfy it. Instead, an iterative, or graphical procedure was used to find values of u and v at a series of points along each streamline. A hodograph plot of the streamlines for $K = 2$ is shown in figure 4. Once the velocity components, u and v, along the

streamlines have been determined, their shape in the physical plane may be found. From (7),

$$x = 2(h+1) - \frac{2(h+1)(u^2-v^2-2hu+1)}{(u^2-v^2-2hu+1)^2+4(hv-uv)^2} - \tfrac{1}{2}\ln\left[\frac{(u^2-v^2+2u+1)^2+4(v+uv)^2}{(u^2-v^2-2hu+1)^2+4(hv-uv)^2}\right] - \frac{K+1}{2(K-1)}\ln\left[\frac{(u-K)^2+v^2}{(uK-K)^2+v^2K^4}\right], \quad (9)$$

$$y = \frac{4(h+1)(hv-uv)}{(u^2-v^2-2hu+1)^2+4(hv-uv)^2} - \frac{K+1}{K-1}\arctan\left[\frac{v(1-K^2)}{K(u^2+v^2-2hu+1)}\right] - \arctan\left[\frac{-2(v+uv)(u^2-v^2-2hu+1)-2(hv-uv)(u^2-v^2+2u+1)}{(u^2-v^2+2u+1)(u^2-v^2-2hu+1)-4(v+uv)(hv-uv)}\right]. \quad (10)$$

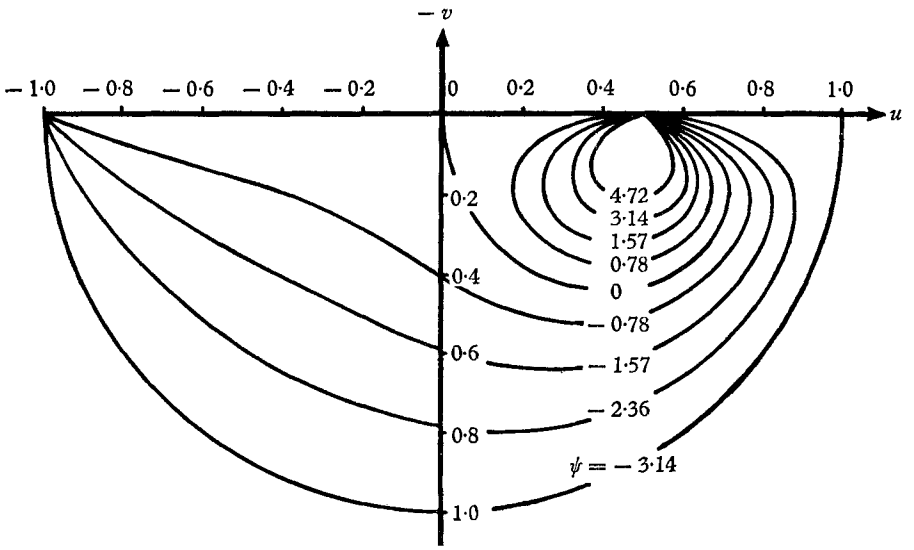

FIGURE 4. Streamlines of flow in hodograph plane for $K = 2$.

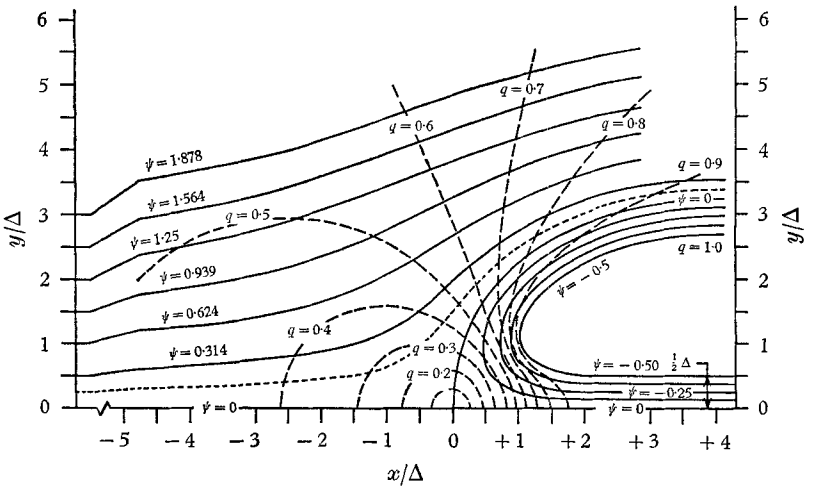

FIGURE 5. Jet penetration streamlines and isovels for flow of $K = 1{\cdot}6$.

The resulting streamline patterns are presented in figures 5 and 6 for K values of 1·6 and 2·5. The x and y scales are here made dimensionless by dividing each scale by the full jet width Δ and the value of ψ on each streamline similarly is divided by Δ.

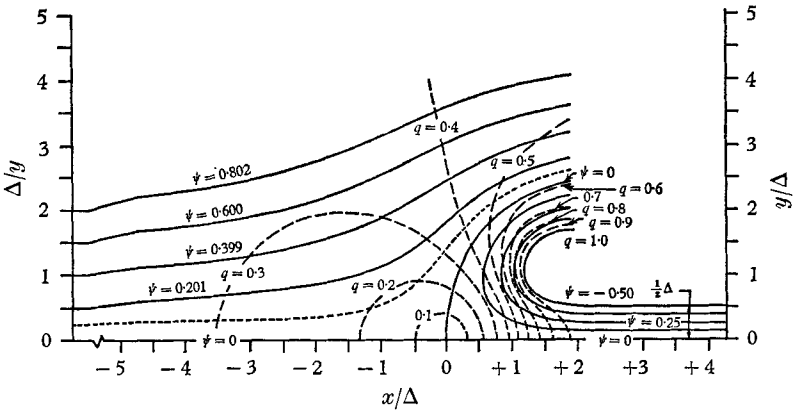

FIGURE 6. Jet penetration streamlines and isovels for flow of $K = 2{\cdot}5$.

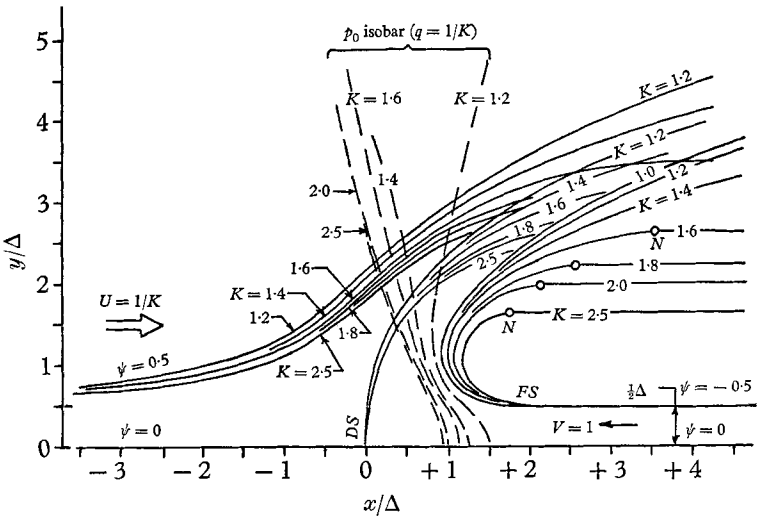

FIGURE 7. Comparison of streamlines at different values of parameter K.

The most significant streamlines of the flow are the free streamline, FS, and the dividing streamline, DS. The shape of these streamlines for all K values considered is shown in figure 7, together with the free streamline for $K = 1$ as obtained by Birkhoff & Caywood (1949). The effect of the value of K on the cavity width is evident from the flow patterns. The ratio of the cavity width W to the jet width Δ is given by

$$\frac{W}{\Delta} = 1 + \frac{K+1}{K-1}.$$

The variation in cavity width with K is shown in the following table.

K =	1·0	1·2	1·4	1·6	1·8	2·0	2·5	3·0
W/Δ =	∞	12	7·0	5·3	4·5	4·0	3·3	3·0

TABLE 1. Variation in cavity width with parameter K

5. Effect of fluid density

The analysis considered up to this point has been purely kinematic, and fluid density enters only when the pressure variation in the flow is desired. This simply results from the assumption that the densities of both the jet and the counterstream are the same. The solution is easily extended to fluids of different densities, however. In such cases, the dividing streamline DS separates the two liquids as a streamline of density discontinuity.

The flows are irrotational and Bernoulli's equation applies throughout each region. Consideration of the mutual stagnation point 0, indicates that the Bernoulli constant (i.e. the stagnation pressure) is identical for both regions. More specifically the pressures on either side of the dividing streamline must be equal; thus

$$(\rho_1 q_1^2)_{DS} = (\rho_2 q_2^2)_{DS}, \tag{11}$$

where the subscript 1 refers to the jet and subscript 2 the counterstream. By definition of the stream function, $q = \partial\psi/\partial n$ with n the normal to the streamline. This expression is substituted into (11) and integrated, whence

$$(\psi_2)_{DS} = (\rho_1/\rho_2)^{\frac{1}{2}} (\psi_1)_{DS}.$$

This relates ψ_2 and ψ_1 along the dividing streamline. Now if ψ is continuous throughout each region there is no limitation to the area near the dividing streamline, thus, throughout the flow region

$$\psi_2 = (\rho_1/\rho_2)^{\frac{1}{2}} \psi_1. \tag{12}$$

It follows directly that the velocity magnitude is also changed by square root of the density ratio,

$$q_2 = (\rho_1/\rho_2)^{\frac{1}{2}} q_1. \tag{13}$$

This general result has been indicated by Birkhoff (1948), Wuest & von Trotha (1964) and Robertson (1965, p. 162).

If a flow exists with jet and counterstream fluids of different density, the streamline pattern is the same as if the fluids were of the same density. Thus ψ_1 can be obtained from the kinematic solution, that is, with the density the same throughout both regions. Once the appropriate value of K has been determined, the streamline pattern is known. The stream function, ψ_2, which describes the flow of the counterstream fluid, is related to ψ_1 by (12) and the velocities in the counterstream are merely changed by the factor $(\rho_1/\rho_2)^{\frac{1}{2}}$ from those given by the kinematic solution. The velocity of the approaching stream is then

$$U = \frac{V}{K}\left(\frac{\rho_1}{\rho_2}\right)^{\frac{1}{2}}. \tag{14}$$

Isovels of the flow pattern (figures 5–7) are still lines of constant pressure. In the jet fluid region the velocity magnitude of the isovels remains unaltered, but in

the stream fluid region the velocity magnitude represented by each isovel is modified by the factor $(\rho_1/\rho_2)^{\frac{1}{2}}$. A discontinuity in tangential velocity across the dividing streamline is thus evident.

6. Experimental studies

Analysis of the penetration problem involves the parameter K which is not defined and can only be determined by experimental methods. Experimental studies were conducted to obtain information on possible values of this parameter. The test conditions were brought as close as possible to the assumptions of the analytical solution. Thus, it was intended that the effects of gravity be minimized and that the flow be approximately two-dimensional. Two types of experiment were conducted corresponding to steady jet penetration into counterstream and unsteady jet penetration into fixed fluid.

In the first type of study, a two-dimensional uniform stream was generated by allowing water to flow between two parallel plates spaced one inch apart vertically. The upper plate was glass, and the lower plate carried a Pitot-static tube which could be positioned at any point in the flow field. The plates were horizontal so that the jet spread in a horizontal plane and the effects of gravity on the flow pattern were minimized. A nozzle inserted between the plates discharged a jet of width $\Delta = \frac{1}{2}$ in. directly into an approaching stream. The test section (8 in. wide) was bounded on both sides by quiescent fluid to simulate a stream of infinite width. The interface between the jet and the stream was made visible by use of black dye in the jet fluid; the free streamlines were marked by concentrated streams of dye released on each side of the nozzle exit. Photographs of the flow pattern obtained through the glass plate served to indicate the shape and position of the DS and FS streamlines although some diffusion of the dyes into the surrounding fluid occurred.

These tests employed water for both the jet and counterstream fluids at jet velocities of 4, 6, 8, 10 and 12 ft./sec. For each jet velocity the counterstream velocity was adjusted to give velocity ratios K of 1·2, 1·4, 1·6, ... until the flow pattern became unstable. At low velocity ratios, the interface appeared close to the nozzle exit, and flow was greatly influenced by the presence of the nozzle. As the velocity ratio K was increased, the interface moved further away from the nozzle until the flow pattern became unsteady with the jet wagging from side to side. This instability suggests that the nozzle then had only minor influence on the flow, so that the situation was then comparable to that of a jet originating at infinity, as assumed in the analysis. Over the range of jet velocities studied, the values of K thus found scattered between 1·71 and 1·77 with an average value of 1·74. This value for the parameter K is the same order of magnitude as that of 1·54 established by Roshko (1954) for the normal plate; of course, there is no particular reason that the values should be the same for the two flow cases.

The general features of the flow agreed well with the theoretical flow model as may be seen in the photograph of figure 8*, plate 1. The dividing streamline between the jet fluid and the stream fluid was well defined with very little mixing

* Some misleading shadows appear in this figure.

along the interface until it became nearly parallel with the nozzle axis. The free streamlines of the jet were in contact with a 'dead water' region. A large eddy and considerable mixing of the jet fluid into these regions resulted, in contrast to the theoretical model. The dividing streamline which formed the interface became parallel to the axis a few nozzle widths downstream of the stagnation point. The final width, from the five tests at $K = 1{\cdot}6$, was 5·8 times the jet width, not far from the value of 5·3 as predicted (table 1).

The velocity was measured at a series of points along the centreline of the test section. When normalized by the jet velocity, nearly identical results were obtained for the five levels of jet velocity tested. The variation for a velocity ratio of 1·6 is indicated in the lower part of figure 8, where each data point represents an average of the five tests. Due to the fluctuation in the position of the stagnation point, accurate velocity measurements were not obtained in the stagnation region. In the counterstream, a good agreement between theoretical and experimental velocity appears. In the jet region the correlation is not as good, and shows that the nozzle still has an appreciable effect on the velocities within the jet.

Penetrated fluid	Specific weight (lb./ft.^{3})	Density ratio. Jet to penetrated fluid	Viscosity centipoises
Gasoline	44·00	1·42	0·43
Castor oil	59·70	1·04	986
Water	62·31	1·00	1·00
Brine	70·33	0·887	1·60
Glycerine	78·60	0·794	1490
Carbon tetrachloride	99·60	0·626	0·969

TABLE 2. Some properties of penetrated liquids used with water jets fluids

For the second type of experiment, the unsteady case of jet penetration was studied by taking motion pictures of water shooting vertically into bodies of initially still liquid. The jet had an initial width Δ of $\frac{1}{2}$ in. and was injected from a nozzle located 2·5 in. above the free surface of the penetrated liquid contained between two vertical glass plates (16 by 20 in.) spaced 1 in. apart. A water jet velocity of $V_j = 10$ ft./sec was produced by a suitable head of water in an upper tank separated from the nozzle by a solenoid-operated, quick-opening valve. Motion pictures taken at 2000 frames/sec served to establish the jet speed before it struck the penetrated liquid and to observe the penetration development. Six different liquids, whose relevant basic properties (at the temperature of test) are indicated in table 2, were employed to vary the density ratio ρ_1/ρ_2 of the jet to penetrated fluid from 0·6 to 1·4. Two of them had viscosities much greater than the others; since no significant divergences from the trend found with the less viscous fluids appeared, an insensitivity of the phenomenon to viscosity is suggested. In all cases, the depth of penetration was found to increase linearly with time for depths as great as 15 times the jet width. Relevant to the steady-state analysis, this penetration velocity is simply

$$V_p = U,$$

while the jet velocity is

$$V_j = V + U.$$

Thus, the jet velocity corresponding to the steady case analysed is $V = V_j - V_p$ whence by (14)

$$V_p = V_j \frac{(\rho_1/\rho_2)^{\frac{1}{2}}}{K + (\rho_1/\rho_2)^{\frac{1}{2}}}. \tag{15}$$

Thus the parameter K is determined from the V_p observations as

$$K = \frac{V_j - V_p}{V_p} \left(\frac{\rho_1}{\rho_2}\right)^{\frac{1}{2}}. \tag{16}$$

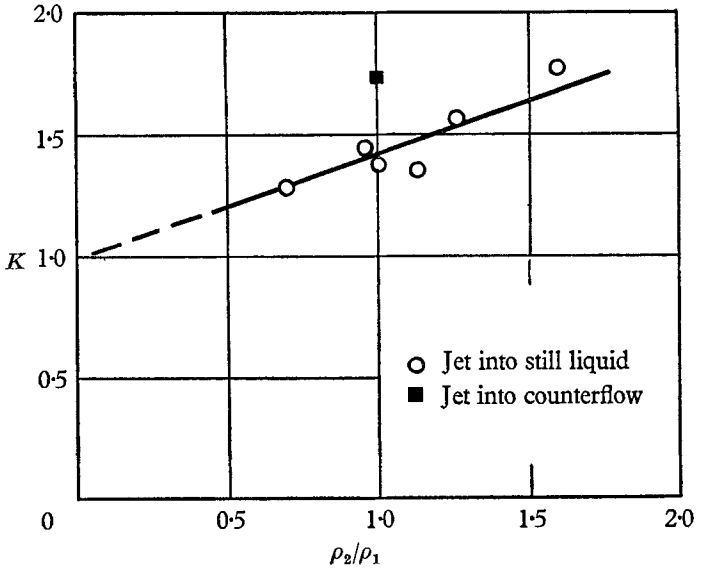

FIGURE 9. Parameter K as a function ratio of density of penetrated to jet fluid.

For a water jet velocity V_j of 10 ft/sec, the observed penetration velocities V_p varied from 4·84 ft/sec in gasoline to 3·08 in carbon tetrachloride, and the K values thus ranged from 1·28 to 1·77. Since the values of this fundamental parameter seem to increase with the inverse of the density ratio and a unity value holds some rationale for an inverse density ratio of zero (as a liquid jet into air), a plot on this basis is presented in figure 9.

Included in figure 9 is the value of K obtained in the steady flow test described earlier. This value is seen to lie significantly above the data for a jet into still fluid. There are two possible reasons for this difference. In the steady flow case the nozzle was closer to the dividing streamline, and may have influenced the flow. The more significant effect, however, is that in the unsteady flow case the space outside the jet was free (actually air filled) whereas in the steady flow study it was filled with water.

The unsteady flow jet penetration studies also yielded information on the shape of the dividing and free streamlines DS and FS for the several density ratios. Some comparisons of the contours of these two important streamlines with

theoretical predictions are given in figure 10 where it is seen that the agreement is quite good, considering the difficulty of exact determination of such streamlines from frames of movie film.

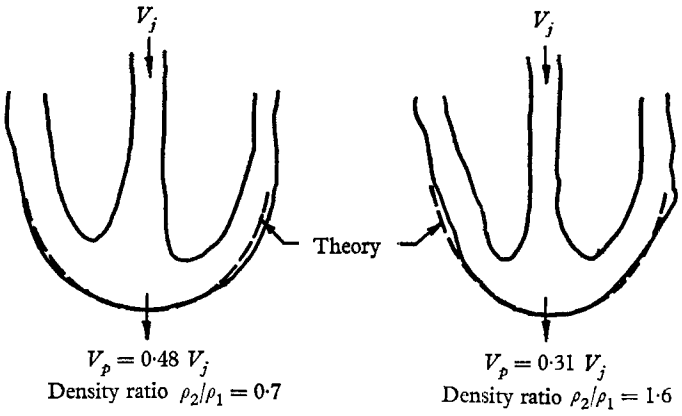

FIGURE 10. Some observed unsteady flow jet boundaries.

7. Conclusions

The most significant feature of the steady-state penetration process with fluids of equal density is that the jet velocity is considerably greater than that of the opposing stream velocity. In the unsteady case of surface penetration, the corresponding condition is that the velocity of penetration is less than one half the jet velocity. The effect of this velocity deficit is to limit the spread of the jet fluid to a finite region along the jet axis. In the analysis, the velocity deficit is accounted for by an empirical parameter, K. Once a suitable value of K has been found, the theory yields velocity and pressure fields and a streamline pattern which correspond reasonably well with experimental observations. For the low range of velocities tested, K does not appear to be sensitive to the magnitude of the jet velocity.

The conditions occurring in the region outside the free streamline influence the value of K. In particular, the value of K obtained when the 'dead water' region occurs appears to be significantly different from that found with liquids when a gas filled cavity exists. In the surface penetration tests (gas-filled cavity) a K value of 1·4 was obtained for the equal density case compared to 1·7 when the cavity was liquid filled. These results suggest that the velocity dissipation along the free streamline is an important factor in determining the flow pattern.

When the jet and stream fluids have different densities, the parameter K increases linearly with the ratio of the density of the penetrated to jet fluid. The flow pattern and the pressure field, for a given value of K, are predicted by theory to be the same as for the equal density case, but in the counterstream, or penetrated fluid region, the velocity components are changed by the square root of the density ratio, stream fluid to jet fluid. A velocity discontinuity then exists at the separating streamline, and mutual boundary layers will develop along the interface which were not accounted for in the theory.

REFERENCES

BANKS, R. B. & BHAVAMAI, A. 1965 Experimental study of the impingement of a liquid jet on the surface of a heavier liquid. *J. Fluid. Mech.* **23**, 229–240.

BANKS, R. B. & CHANDRASEKHARA, D. V. 1963 Experimental investigation of the penetration of a high-velocity gas jet through a liquid surface. *J. Fluid Mech.* **15**, 13–34.

BARON, J. R. & ALZNER, E. 1963 An experimental investigation of a two-layer inviscid shock cap due to blunt-body nose injection. *J. Fluid Mech.* **15**, 442–45.

BIRKHOFF, G. 1948 Remarks on streamlines of discontinuity. *Rev. Cienc. Lima, Peru,* **50**, 105.

BIRKHOFF, G. & CAYWOOD, T. 1949 Fluid flow patterns. *J. Appl. Phys.* **20**, 646.

BIRKHOFF, G., MACDOUGALL, D. P., PUGH, E. M. & TAYLOR, G. I. 1948 Explosives with lined cavities. *J. Appl. Phys.* **19**, 563.

CHARCZENKO, N. & HENNESSEY, K. W. 1961 Investigation of a retro-rocket exhausting from the nose of a blunt body into a supersonic free stream. *NASA TN* D-751.

EHRICH, F. F. 1953 Penetration and deflection of jets oblique to a general stream. *J. Aero. Sci.* **20**, 99–104.

EICHELBERGER, R. J. 1956 Experimental test of the theory of penetration of metallic jets. *J. Appl. Phys.* **27**, 63.

HOPKINS, D. F. 1962 A study of fluid jet penetration. Ph.D. thesis, Dept. of Mechanical Engineering, Univ. of Illinois, Urbana.

LEE, DANA 1932 Experiments on the distribution of fuel in fuel sprays. *NACA Rept.* no. 438.

MILLER, H. E. & BEARDSLEY, E. G. 1926 Spray penetration with a simple fuel injection nozzle. *NACA Rept.* no. 22.

PACK, D. C. & EVANS, W. M. 1951 Penetration by high velocity jets. *Phys. Soc. Proc.* B **64**, part 4.

RAO, T. R. K. 1958 Investigation of the penetration of a jet into a counterflow. M.S. thesis, Dept. of Mechanics and Hydraulics, University of Iowa, Iowa City.

ROBERTSON, J. M. 1965 *Hydrodynamics in Theory and Application.* Englewood Cliffs, N.J.: Prentice-Hall.

ROMEO, D. J. & STERRETT, J. R. 1963 Exploratory investigation of the effect of a forward-facing jet on the bow shock of a blunt body in a Mach number 6 free stream. *NASA TN* D-1605.

ROSHKO, A. 1954 A new hodograph for free-streamline theory. *NACA TN* 3168; also 1955 On the wake and drag of bluff bodies. *J. Aero. Sci.* **22**, 124–32.

SINGH, S. 1957 Penetration by high-speed metallic jets. *Proc. Phys. Soc.* **70**, B, 867.

STALDER, & INOUYE, M. 1956 A method of reducing heat transfer to blunt bodies by air injection. *NACA RM* A 56 B 27*a*.

WARREN, C. H. E. 1960 An experimental investigation of the effects of ejecting a coolant gas at the nose of a bluff body. *J. Fluid Mech.* **8**, 400–17.

WUEST, W. & VON TROTHA, H. 1964 Reibungslose Strömung an Flügelnasen mit Ausblasen eines anderen Gases. *J. Mécanique,* **3**, 323–43.

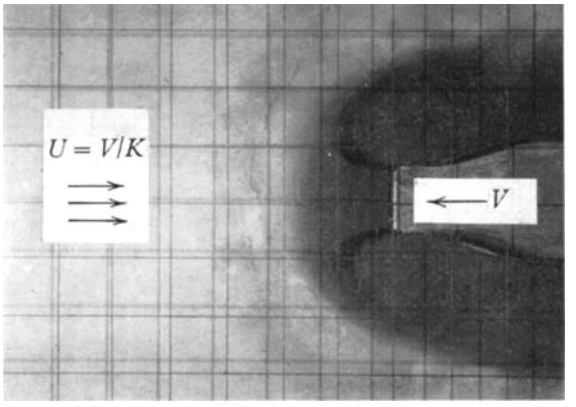

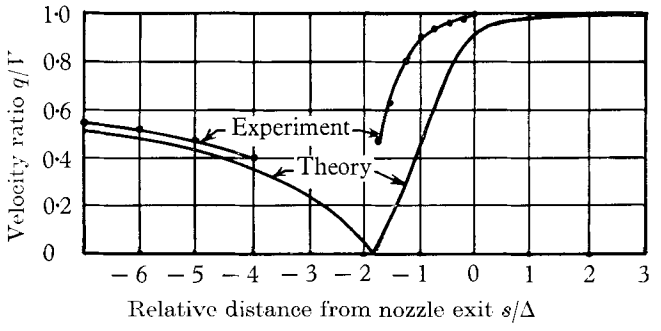

FIGURE 8. Flow pattern and velocity variation along centreline for counterflow at $K = 1{\cdot}6$.